Glueballs and topology in lattice QCD with two light flavors

Khalil M. Bitar, R. Edwards, U. M. Heller, and A. D. Kennedy
Supercomputer Computations Research Institute, The Florida State University, Tallahassee, Florida 32306-4052

Thomas A. DeGrand
Physics Department, University of Colorado, Boulder, Colorado 80309

Steven Gottlieb and A. Krasnitz
Department of Physics, Indiana University, Bloomington, Indiana 47405

J. B. Kogut and R. L. Renken
Department of Physics, University of Illinois, 1110 W. Green St., Urbana, Illinois 61801

W. Liu and Pietro Rossi
Thinking Machines Corporation, Cambridge, Massachusetts 02142

Michael C. Ogilvie
Department of Physics, Washington University, St. Louis, Missouri 63130

D. K. Sinclair and K. C. Wang
High Energy Physics Division, Argonne National Laboratory, 9700 S. Cass Ave., Argonne, Illinois 60439

R. L. Sugar
Department of Physics, University of California, Santa Barbara, California 93106

Michael Teper
All Souls College and Department of Theoretical Physics, University of Oxford, Oxford OX1 3NP, United Kingdom

D. Toussaint
Department of Physics, University of Arizona, Tucson, Arizona 85721

(Received 4 February 1991)

We obtain estimates of the lightest glueball masses, the string tension, and the topological susceptibility in an exploratory study of QCD with two light flavors of quarks. Our calculations are performed at $\beta=5.6$ with staggered quark masses $m_q=0.010$ and 0.025 and on lattices ranging from 12^4 to 16^4. Our estimates suggest that, just as in the pure gauge theory, the 0^{++} is the lightest glueball with the 2^{++} about 50% heavier. Our $m_q=0.01$ results predict a 0^{++} glueball mass of about 1.6 times the ρ mass and the square root of the string tension of about 0.48 times the ρ mass, which is surprisingly close to the usual phenomenologically motivated estimates of around 0.55. Our value of the topological susceptibility at $m_q=0.01$ is consistent with the prediction, to $O(m_q)$ of the standard anomalous Ward identity. However, the variation of this susceptibility between $m_q=0.01$ and $m_q=0.025$ is weaker than the linear dependence one expects at small m_q in the broken-chiral-symmetry phase of QCD.

I. INTRODUCTION

Lattice QCD presents us with a tool to calculate the hadron spectrum from first principles. In addition to allowing the calculation of the low-lying meson and baryon states, which would ultimately test QCD, it also allows us to determine the fate in full QCD of the pure glue states (glueballs) which make up the spectrum in the absence of quarks and for which the experimental situation is still confused [1]. Should lattice QCD point to the presence of relatively pure glueball states and give their masses, this would greatly clarify the experimental situation. The verification of any such predictions would be a crucial test of QCD, since they depend on the gluonic sector which distinguishes QCD from simple quark models. To date the only convincing lattice-gauge-theory calculations of glueball masses have been in pure gauge theories without the presence of dynamical quarks [2–4]. The primary purpose of the present paper is to begin the process of obtaining equally reliable calculations of "glueball" masses in full QCD.

Including light dynamical quarks in the glueball calculations changes things in two important ways. First there

 ©1991 The American Physical Society

will be mixing between glueballs and mesons and this will alter the level pattern that one observes in the pure gauge theory. Indeed the level pattern may undergo large changes irrespective of the amount of mixing because the vacuum itself is qualitatively altered by the presence of light quarks. Second, even if the level pattern is not grossly altered, the simultaneous calculation of states such as the ρ meson enables us to assign values in GeV units to the "glueball" masses, something which is not really possible in the pure gauge theory. Of course, if the mixing is large then the lattice calculations will inevitably encounter some of the same difficulties that experiments do in attempting to identify the glueball spectrum. Even in this case, however, lattice calculations possess what is likely to be a crucial advantage over the "real world:" parameters can be varied away from their physical values in such a way as to smoothly reduce some of the obscuring phenomena. For example, increasing the quark masses will gradually reduce the mixing, and perhaps more importantly increase the pion mass thereby inhibiting "decays." Decreasing the volume can also prevent some states from "decaying." In any case, the present exploratory calculation is not accurate enough to confront us with the challenge of having to resolve such difficulties. Indeed, as we will see, the reliability of our estimates of glueball masses depends, in practice, on the mixing being small: if it is not small then our numbers merely provide upper bounds on the lightest masses in the appropriate channels. Although we have not attempted a direct calculation of meson-glueball overlaps (a lacuna which we intend to correct in future work) we do have some indirect handle on the mixing. In particular by calculating glueball masses both at a larger quark mass (in lattice units), $m_q=0.025$, where any mixing is likely to be small, and at a lower mass, $m_q=0.010$, where it could well be sizable, and by comparing these with the older quenched data, we can search for the changes in the (apparent) glueball level spectrum that would (probably) accompany the onset of any substantial mixing.

In addition to calculating glueball masses we shall also calculate the mass of the lightest periodic flux loop, i.e., the loop of color-triplet flux that closes on itself through one of the periodic spatial boundaries. Such a mass can be calculated [2] from correlations of operators of the same type as Polyakov loops and/or Wilson lines whose mass per unit length is simply the string tension. Of course, it is not *a priori* clear that there are going to be any such flux loops once the vacuum acquires light-quark loops. We shall, for now, ignore this important point but shall return to it, nearer the end of the paper, after we have presented all the details of our calculations.

Another focus of our work in this paper concerns topology. The nontrivial topological structure of non-Abelian gauge theories [5,6] is closely associated with the detailed dynamics of QCD. In particular, through the U(1) anomaly it gives the large η' mass [7,8] and contributes to η decay. It has also been implicated in spontaneous chiral-symmetry breaking and hadronic structure [9]. Topological fluctuations can play such roles because they are very sensitive to the presence of light quarks. Thus the question whether the density of such fluctuations is in accord with our theoretical expectations [10] is interesting and one which we shall pursue further in this paper.

We turn now to a brief resume of various technical details concerning our simulations. We simulate lattice QCD with two degenerate flavors of quarks using the hybrid molecular dynamics method. We have run simulations with quark masses $m_q=0.025$ and $m_q=0.010$ on 12^4, $12^3\times 24$, and 16^4 lattices. Low-lying meson and baryon masses have been calculated and reported elsewhere, along with more details of the simulations [11,12].

For our glueball and topological charge calculations we have used 500 equilibrated configurations on a 12^4 lattice with $m_q=0.025$, and another 500 with $m_q=0.010$. In addition we have used 100 configurations on a $12^3\times 24$ lattice and 125 on a 16^4 lattice, each with $m_q=0.010$. Here all consecutive configurations are separated by ten time units. For the 12^4 and 16^4 lattices we have improved our effective statistics by calculating the glueball propagators with all four possible choices of the "time" direction. For the 16^4 lattice we have also calculated a restricted number of states on 1250 configurations separated by only one time unit (using what we shall call "inline code"). For purposes of the error analysis we have binned our data into 20 or 25 bins: thus the bin size was 20 configurations for the 12^4 lattice and 5 for the 16^4 lattice.

Given our limited statistics, a crucial ingredient in our glueball calculations was the use of extended "fuzzy" wave functions [2,13] which have a large overlap onto the low-lying states of interest. However, even with the improved signal-to-noise ratio this gave, we were still restricted to measuring propagators at small separations, in part due to statistics and in part due to the sensitivity of some of our states to modes of the system with very long relaxation times. The only states which gave signals which we could measure with any reliability were the 0^{++} and 2^{++} glueballs and the "fuzzy" Wilson-Polyakov line (which gives an estimate of the lowest mass periodic flux loop and hence of the string tension).

The topological charge of a given lattice gauge field configuration was calculated by the cooling method [14], where the gauge configuration is smoothed locally by bringing each link into contact with a $\beta=\infty$ heat bath, and iterating this procedure. This is designed to remove small topological excitations which are lattice artifacts. The topological charge was found to be sensitive to the long time behavior of the system (as, indeed, was the string tension).

We finish now with a summary of the rest of the paper. In Sec. II we describe the "fuzzy" glueball wave functions which we have used to construct "good" glueball and flux-loop wave functionals. Section III describes in detail the cooling method for calculating the topological charge and summarizes the theoretically expected behavior of the topological susceptibility. Section IV presents the results of our calculations of glueball masses and the string tension, while Sec. V present the results of our topological charge calculation. In Sec. VI we return to a discussion of the effects, if any, of quark loops and mixing on the glueball spectrum and on the string tension. Finally, in Sec. VII, we present our conclusions.

II. IMPROVED GLUEBALL WAVE FUNCTIONS

Simple glueball wave functions, such as the plaquette, have the disadvantage that they only have small overlaps with the lowest-lying glueball states, and that these overlaps become rapidly smaller as the lattice spacing is decreased. This situation can be improved by considering larger Wilson loops as wave functions and by performing a variational calculation. However, in practice any improvement is limited because only a very restricted set of trial wave functions can be included easily. In response to these problems methods have recently been developed to define "smeared" or "fuzzy" wave functions which are extended objects that are linear combinations of large numbers of Wilson loops and have a large overlap with low-lying glueball states [2–4,13,15,16]. Such choices are typically inspired by renormalization-group methods. We have used the version of [2,13].

The need for such improvements to glueball wave functions becomes painfully obvious, in the present calculations, when one considers the behavior of a zero-momentum glueball propagator $C(T)$ where T is the time separation on the lattice. Ignoring, for the moment, the effects of the finite lattice extent in the time direction, we can perform the usual energy decomposition on $C(T)$ and obtain

$$\frac{C(T)}{C(0)}=\sum_n A(n)\exp[-E(n)T]\ , \quad \sum_n A(n)=1\ ,$$
$$\sim A\exp(-MT)\ , \quad A\leq 1 \tag{2.1}$$

at large T, where A is a constant and M is the mass of the lightest (glueball?) state in that channel. A represents the magnitude squared of the projection of the glueball wave function on to this lowest-lying state, and would thus be 1 if there were no contamination from higher-mass states. Thus the closer A is to 1, the less the contamination from excited states, and the smaller the T values at which this asymptotic form is a good approximation. If we make a total of N independent measurements, we can only hope for a sensible determination of this mass provided the signal is much larger than the error, i.e.,

$$Ae^{-MT}\gg 1/\sqrt{N}\ . \tag{2.2}$$

hence we need A to be as close to unity as possible, so that M can be extracted from as small T as possible.

The scheme we use [2,13] is based on defining "blocked" or "fuzzy" links by

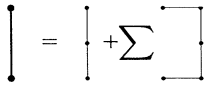

(2.3)

where the sum is over the four "staples" in the two spatial directions orthogonal to the direction of the blocked (spatial) "link." This link matrix is then projected back into SU(3); that is, if A is the blocked link of the left-hand side of equation (2.3), we replace it with the SU(3) matrix U which maximizes $\mathrm{Re\,Tr}(UA^{\dagger})$. This maximization is performed by a method analogous to a Cabibbo-Marinari heat bath with $\beta=\infty$. A single sweep of the lattice was found to suffice, in that the ratios $C(T)/C(0)$ obtained in this approximation are in agreement with those for the exact maximation. Higher levels of blocking are obtained by iterating this procedure. Thus the 0th-level blocked link (unblocked) has length 1, the first length 2, the second 4, the third 8, etc. These blocked links are used to create wave functions of a given template, e.g., a "plaquette," or a Wilson-Polyakov "line." We have considered templates consisting of the 1×1 loop (which we shall frequently refer to as a plaquette despite the fact that its actual size in lattice units is 2^N, where N is the blocking level, a 1×2 rectangular loop, a six-link nonplanar loop and an eight- link nonplanar loop. These are shown in Fig. 1. The wave functions with particular spin-parity assignments are obtained by appropriate linear combinations of different orientations of such loops. For details we refer the reader to Ref. [2]. For example, the two $1\times 2, 2^{++}$ wave functions denoted $1\times 2L$ and $1\times 2S$ are from subtracting 1×2 rectangular loops differing by rotations of $\pi/2$ about the long and short axes of the rectangle, respectively. The spin-parity-charge conjugation combinations thus obtained are

$$0^{++}\ 0^{+-}\ 0^{-+}\ 0^{--}\ ,$$
$$1^{+-}\ 1^{-+}\ , \tag{2.4}$$
$$2^{++}\ 2^{+-}2^{-+}2^{--}\ ,$$

and higher spin states. In the case of the Wilson-Polyakov line, we use only one template, the straight line of links in one of the spatial directions, closed through the periodic boundary. The only complication occurs when the spatial extent of the lattice is not an integer power of 2. In that case we take products of different blocked links. For example, in the case of the 12^4 lattice we define the blocking-level-3 Polyakov loop by multiplying a level-3 link (length 8) with a level-2 link (length 4). Note also that where necessary we explicitly subtract the vacuum expectation value from our operator.

In addition to considering states of zero momentum we also calculate states of nonzero momentum. There are several reasons to do so: (a) we would like to test the extent to which the continuum dispersion relation

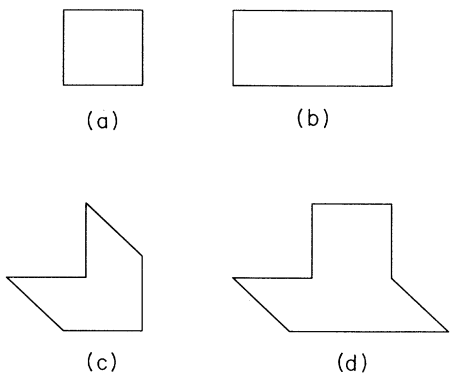

FIG. 1. Templates for blocked glueball wave functions: (a) a 1×1 loop; (b) a 1×2 loop; (c) a six-link nonplanar loop; (d) an eight-link nonplanar loop.

$E^2=p^2+m^2$, has been restored: this would provide one measure of the extent to which Lorentz invariance has been restored; (b) once the continuum dispersion relation is well established then one can combine the $p=0$ and $p\neq 0$ data to improve statistics; (c) it is frequently hard to tell if some apparent "anomalous" behavior of $p=0$ propagators at large T is real or merely a product of underestimating the statistical errors once they are large: a comparison with $p\neq 0$ propagators can frequently be illuminating in these cases; (d) in small volumes the masses obtained using $m^2=E^2-p^2$ differ strongly from the masses obtained from $p=0$ propagators: this is, in practice, a sensitive indicator of the fact that the volume is becoming small.

Wave functions of spatial momentum $\mathbf{p}$ are obtained by associating each loop with a single point on the lattice, then summing over the loops associated with each point on the fixed T hyperplane weighted by $\exp(i\mathbf{p}\cdot\mathbf{x})$ where $\mathbf{x}$ is the lattice point associated with the particular loop. Denoting such a wave function by $W(\mathbf{p},T)$, our glueball propagator $C(\mathbf{p},T)$ is given by

$$C(\mathbf{p},T)=\frac{1}{V}\left\langle \sum_t W^\dagger(\mathbf{p},t)W(\mathbf{p},t+T)\right\rangle , \tag{2.5}$$

where V is the space-time volume of the lattice and $\langle\ \rangle$ represents an average over the ensemble of gauge field configurations. In practice our fuzzy operators become less efficient as p is increased. This is not surprising because the "blocking" algorithm was originally tuned to work well for the low-lying $p=0$ states [2,13]. This has the practical consequence that in order to extract the energy of the lightest glueball one has to go to larger T along the corresponding propagator as p is increased. However, since $E(p)$ increases with p, the correlation function will descend more rapidly into the "noise" with increasing T for larger p. All this can obviously introduce systematic biases when we extract $E(p)$ in calculations of limited statistics, such as ours. For these reasons we shall use, in our final averages, only masses that are extracted from $p=0$ or the lowest nonzero value of p.

In practice we have limited ourselves to the smallest nonzero momenta because once the momentum and energy become large the signal disappears too rapidly to be useful. For the 0^{++} wave functions based on the 1×1 loop we have calculated the propagator with one spatial component of momentum nonzero and equal to $2\pi/L$, with L the spatial dimension of the lattice (this being the lowest nonzero momentum allowed) and also the propagators with two spatial components of momentum nonzero and equal to $2\pi/L$. For the 2^{++} plaquette wave function we have also calculated the propagators with the component of the momentum in the direction common to the two plaquettes defining this wave function equal to $2\pi/L$. This ensures that the momentum is parallel to the spin so that when boosted back to its rest frame this supposedly 2^{++} wave function does not acquire any 0^{++} component. For the spatial Wilson-Polyakov line we have calculated the propagators with one or both of the spatial components of momenta orthogonal to the line's orientation, equal to $2\pi/L$.

We end this section with some general remarks on our above iterative scheme. Its purpose is to construct in an efficient way large smooth wave functions. Good wave functions need to be large so as to match the expected $\sim$1-fm size of physical glueballs and they should be smooth because that is the simplest expectation for ground states. One would hope, ideally, that if the lattice spacing is reduced by a factor of 2, all one needs to do is iterate the procedure just once more and use the same template as before to obtain an equally good wave function. In the pure gauge calculations this does indeed turn out to be the case [2]. Moreover the best wave function that one builds in this way typically has $A>0.8$ (in the pure gauge case) so that one can already obtain a good approximation to M from $C(2)/C(1)$. Of course once we allow glueball states to mix with $q\bar{q}$ states this may all change. It is only if this mixing is reasonably small that we can expect A for the best such gluonic operator to be large; if the mixing is large—and between several states—then A will almost certainly be well below $\frac{1}{2}$. Since statistics limits us, in the present work, to masses extracted from $t<3$ it is only in the former case of small mixing that our effective masses are likely to be any approximation at all to the true masses.

III. TOPOLOGICAL CHARGE BY THE COOLING METHOD

The topological charge of a gauge field acquires ambiguities when space-time is discretized. Nonetheless we expect that as the lattice spacing is made to vanish these ambiguities will also vanish: at least as far as the long-distance physical properties of topology are concerned. We expect this because we know from standard semiclassical calculations that the density of instantons decreases very rapidly as the instanton scale size ρ decreases. This argument does, however, break down once $\rho\sim 1$ (in units of the lattice spacing): as ρ is reduced to zero the gauge-invariant core of the instanton shrinks within a hypercube and disappears from the lattice. At the same time the field configuration interpolates smoothly between $Q=1$ and $Q=0$ and the action between $S=8\pi^2/g^2$ and $S=0$. Although the density of such configurations may be large they are irrelevant to the physics of topology: the associated zero modes, for example, are in fact far from zero. Nevertheless they pose an obvious complication for any attempt to calculate the topological charge on the lattice. A further complication arises when we attempt to define a lattice topological charge density: such a composite field operator, if applied to rough lattice gauge fields, is inevitably dominated by ultraviolet fluctuations.

A simple way to obtain a topological charge from a given rough lattice gauge field that is insensitive to the above lattice artifacts is to first smooth out the local fluctuations of the given lattice field. Such a local smoothing can be achieved by altering the field configuration one link at a time in such a way as to minimize the piece of the action that involves that link. This procedure can be repeated and a finite iteration of it will leave unaltered the physical component of the global topology if the lattice spacing is small enough. This is because, in the con-

tinuum, sectors of differing topological charge are separated by infinite action barriers which cannot be breached by "local smoothing." The following remarks should serve to clarify this last assertion. First we observe that on the lattice of lattice spacing a the finite remnants of these barriers are provided by the fact that the action of an instanton whose core is a few lattice spacings across is

$$S \approx \frac{8\pi^2}{g(a)^2} \rightarrow \infty, \quad \text{as } a \rightarrow 0 \tag{3.1}$$

where $g(a)$ is the running coupling constant on a size scale of one lattice spacing. (Technically speaking, to have a barrier one requires that the action of such an instanton diverge fast enough as $a \rightarrow 0$ for the diverging density of states factor, $1/a^4$, to be overwhelmed by the vanishing e^{-S} factor. This indeed happens to be the case for non-Abelian gauge theories in four dimensions.) Now, to change the lattice topological charge on physical length scales, via a local procedure, requires that an (anti-)instanton grows or shrinks through size scales of a few lattice spacings. Because of the diverging action of such instantons, the probability that this should happen in, for example, a Monte Carlo–generated sequence of configurations goes rapidly to zero as $a \rightarrow 0$ and so the sequence becomes locked into a given topological charge sector. Thus, as $a \rightarrow 0$ the physical topological charge of a typical lattice field resides in cores that are on a length scale $\gg a$. In addition to this topological charge, there are "instantonlike" lattice fluctuations on size scales $\rho \lesssim a$ whose action has been sufficiently reduced by the discretization that it is not large enough to control the $1/a^4$ density of states factor. (These effects are clearly not universal and depend on details of the lattice action.) These objects are lattice artifacts in the sense that they do not affect fermionic (or other) physics on physical length scales. Thus we would exclude them from our calculations. Now if we locally smooth (cool) such a lattice gauge field, in the way described earlier in this paragraph, then these lattice artifacts with $\rho \lesssim a$ will shrink out of the lattice in the first few iterations of the smoothing procedure. On this time scale the physical topology will hardly shrink at all, and will certainly not shrink right out of the lattice. This is, of course, because $\rho \gg a$ for such charges. Moreover the shrinking of these instantons is driven by $O(a^2/\rho^2)$ corrections to the instanton action which become increasingly weak as $a \rightarrow 0$ in physical units.

Clearly such a smoothing or "cooling" method is unambiguous only if the lattice is large enough and the lattice spacing small enough so that the short- and long-distance fluctuations are well separated and the action barriers separating the sectors of differing physical topological charge are large. Our calculations here are not, of course, performed in this ideal limit, but all the evidence is that the degree of ambiguity is not intolerable.

In practice we follow [14] and perform the local smoothing by minimizing the plaquette action of the gauge field (see [10] for a discussion of this choice action). This is achieved by updating the lattice gauge field in question using a Cabibbo-Marinari heat bath at $\beta(=6/g^2)=\infty$. One such sweep through the lattice is usually referred to as one "cooling sweep." Typically, after a few cooling sweeps ultraviolet fluctuations contributing to the topological charge are almost wholly removed and what remains can be considered to be the physical artifact-free topological charge of the original configuration (provided the original β is large enough for there to be a clear separation between lattice and physical length scales).

If the number of cooling sweeps employed is small then we can expect, in addition, that the topological charge density on the cooled lattice is a reliable reflection of the distribution of the physical topological charge in the original "hot" configuration. The reason for this is that the cooling is a local procedure and, just like a Monte Carlo heat bath, can only create (or destroy) coherent structures over long distances after a sufficiently large number of sweeps.

To calculate the topological charge Q of a smoothed configuration we recall that, in the continuum,

$$Q = \frac{1}{32\pi^2} \int d^4x \, \epsilon_{\mu\nu\rho\sigma} \operatorname{Tr}(F_{\mu\nu} F_{\rho\sigma}) \, . \tag{3.2}$$

On the lattice we replace this with

$$Q = \frac{1}{32\pi^2} \sum_{\text{sites}} \epsilon_{\mu\nu\rho\sigma} \operatorname{Tr}(U_{\mu\nu} U_{\rho\sigma}) \tag{3.3}$$

where U is a product of the SU(3) matrices representing our gauge fields around a plaquette in the $\mu\nu$ plane. This operator has the required continuum limit, and the smoothness of the cooled fields makes it a good approximation, even on fairly coarse lattices.

From Q we calculate the topological susceptibility

$$\chi = \frac{1}{V} \langle Q^2 \rangle \tag{3.4}$$

where V is the space-time volume of the lattice. The anomalous Ward identity for the flavor-singlet axial-vector current requires χ to obey [8,10,17]

$$\chi = \frac{m}{n_f^2} \langle \bar{\psi}\psi \rangle - \frac{m^2}{n_f^2} \chi_p \tag{3.5}$$

even at finite volume, where

$$\chi_p = \int d^4x \, \langle \bar{\psi}(x) i\gamma_5 \psi(x) \bar{\psi}(0) i\gamma_5 \psi(0) \rangle \, . \tag{3.6}$$

For light quarks of mass m in the chirally broken phase, the leading $O(m)$ contribution to χ is

$$\chi = \frac{m}{n_f^2} \langle \bar{\psi}\psi \rangle \, . \tag{3.7}$$

At infinite volume, we would evaluate $\langle \bar{\psi}\psi \rangle$ at $m=0$ to avoid having to define a subtraction scheme to remove the (perturbative) divergences at $m \neq 0$. [Note that the difference between using $\langle \bar{\psi}\psi \rangle$ at zero mass or the subtracted version at mass m contributes a piece of $O(m^2)$ to Eq. (3.5) and so is of the same order as other terms we have neglected.] For a large volume, we can extrapolate $\langle \bar{\psi}\psi \rangle$ to $m=0$, provided the finite-volume corrections of

Hansen-Leutwyler [17] are not too large. This extrapolated $\langle \bar{\psi}\psi \rangle$ would be close to the infinite-volume value at $m=0$, and thus distinct from the finite-volume value at $m=0$, which is zero.

For contrast, in the chirally symmetric phase we would expect

$$\chi \propto m^{n_f} , \tag{3.8}$$

where n_f is the number of light-quark flavors.

IV. GLUEBALL AND STRING TENSION CALCULATIONS

We have calculated the zero- and nonzero-momentum propagators for the wave functions mentioned in Sec. II, for blocking levels 0–3. Figure 2 shows the normalized propagators for the 0^{++} and 2^{++} plaquette wave functions and the Polyakov loop, as a function of T for various blocking levels (all on 12^4 at $m_q=0.025$). Just as in the case of the pure gauge theory we see that blocking

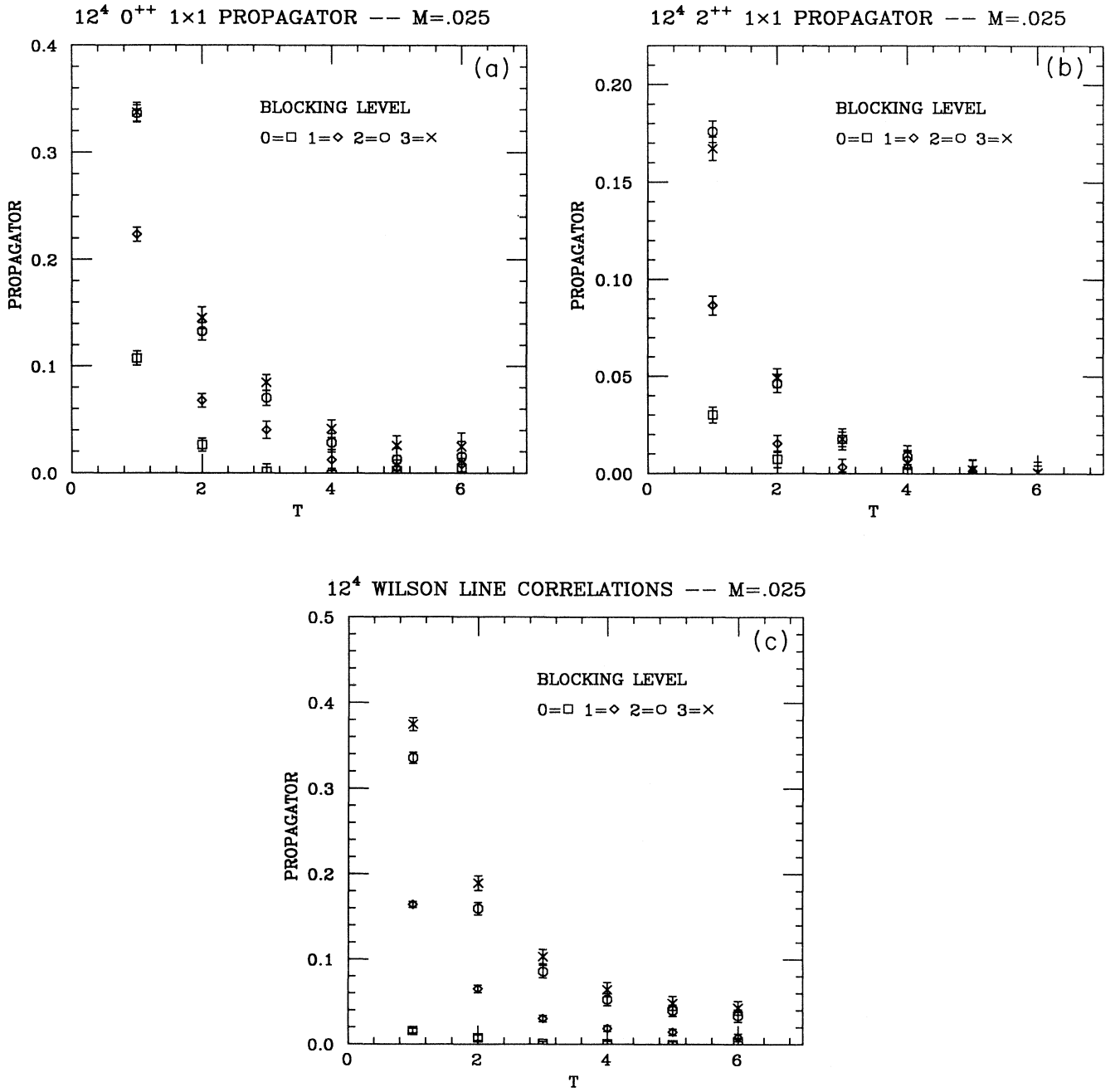

FIG. 2. A linear plot as a function of blocking level. Blocking level zero is unblocked. All on the 12^4 lattice with $m_q=0.025$. (a) The $0^{++}1\times1$ loop propagator. (b) The $2^{++}1\times1$ loop propagator. (c) The Wilson-Polyakov line correlation function.

has greatly improved the signal-to-noise ratio by enhancing the overlap between the chosen wave function and the lowest-lying gluonic states. The similarity between levels 2 and 3 indicates that higher levels of blocking are unnecessary. These features are characteristic of the results on our other lattices and quark masses as well.

In Figs. 3–5 we show the best plaquette propagators for the 0^{++} and 2^{++} glueballs and for the Polyakov loop, respectively. [Recall that, as is conventional in these kinds of calculations, "best" means the one with the largest value of C(1)/C(0).] In each case we show propagators from the 12^4 lattices at both $m_q=0.010$ and $m_q=0.025$. As is apparent, our accuracy rapidly deteriorates for $T>2$ and we know, from pure gauge cal-

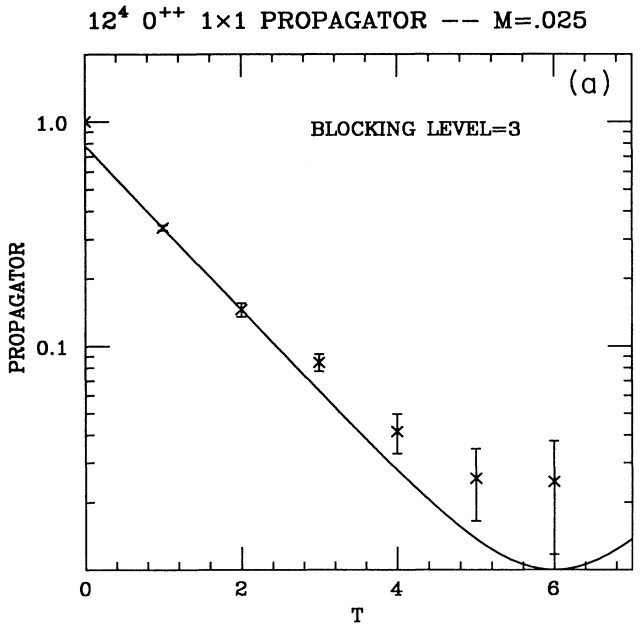

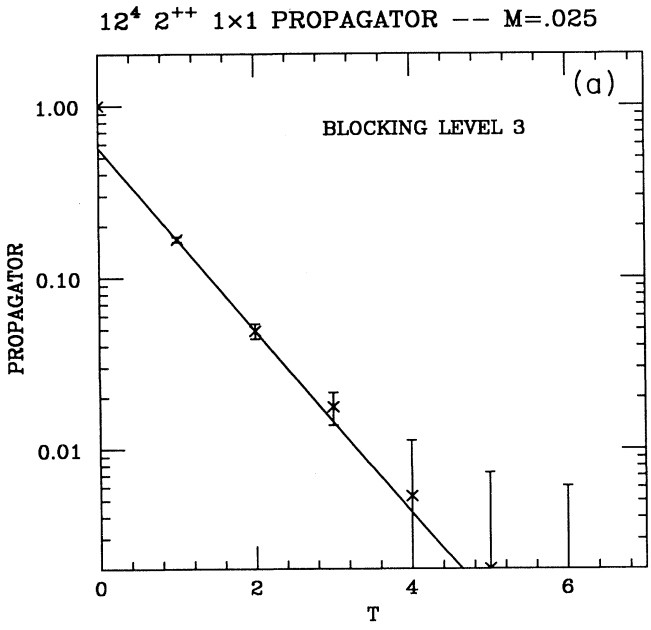

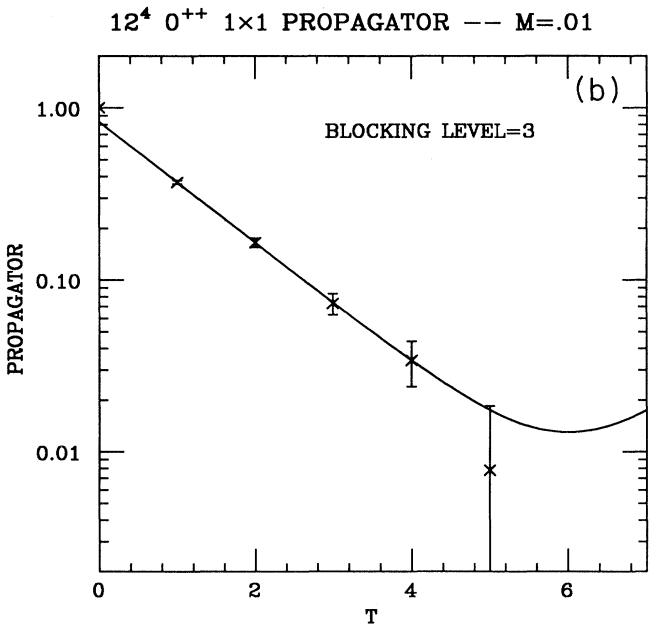

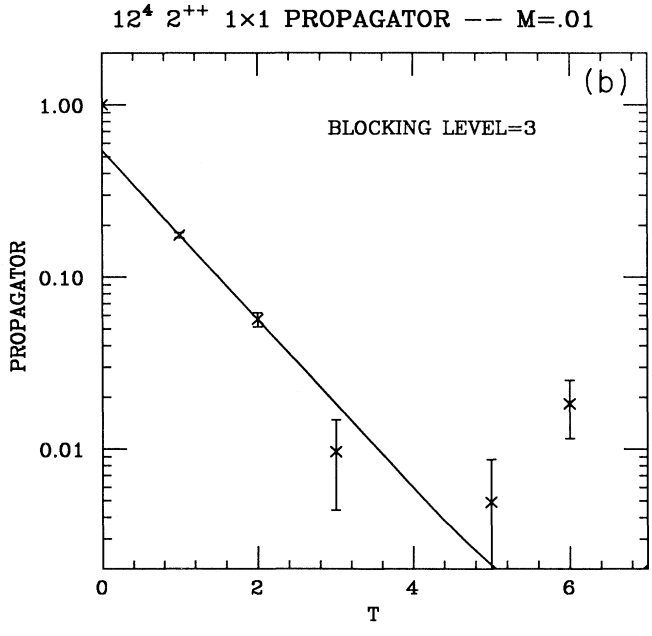

FIG. 3. The $0^{++}1\times1$ loop propagator on a 12^4 lattice: (a) $m_q=0.025$. Blocking level 3 on a logarithmic scale. The fit is to the form $0.7829\{\exp(-0.8422T)+\exp[-0.8422(12-T)]\}$ which fits the $T=1$ and $T=2$ data points. (b) $m_q=0.010$. Blocking level 3 on a logarithmic scale. The fit is to the form $0.8298\{\exp(-0.8080T)+\exp[-0.8080(12-T)]\}$ which fits the $T=1$ and $T=2$ data points.

FIG. 4. The $2^{++}1\times1$ loop propagator on a 12^4 lattice: (a) $m_q=0.025$. Blocking level 3 on a logarithmic scale. The fit is to the form $0.5688\{\exp(-1.2256T)+\exp[-1.2256(12-T)]\}$ which fits the $T=1$ and $T=2$ data points. (b) $m_q=0.010$. Blocking level 3 on a logarithmic scale. The fit is to the form $0.5438\{\exp(-1.1303T)+\exp[-1.1303(12-T)]\}$ which fits the $T=1$ and $T=2$ data points.

culation [18], that once an error becomes large it is usually badly underestimated (due in part to the breakdown of simple, quadratic error analysis, and in part to the fact that at large T where the errors are large, autocorrelation times are also large). Thus we find it convenient to extract local effective masses $m(T)$ from along the correlation functions, rather than relying on global fits. We do this as follows: we fit our glueball propagators locally in T to the asymptotic form

$$C(T)=A\{\exp(-MT)+\exp[-M(N_t-T)]\} \tag{4.1}$$

and calculate the effective mass $m(T)$ by solving

$$\frac{\exp[-m(T-1)]+\exp[-m(N_t-T+1)]}{\exp(-mT)+\exp[-m(N_t-T)]}=\frac{C(T-1)}{C(T)} . \tag{4.2}$$

The errors in $m(T)$ are estimated using the jackknife procedure on our binned data. $m(T)$ should approach M as $T\to\infty$, so ideally we should look for a plateau in $m(T)$ as T increases. Unfortunately for the statistics we have, errors become large before such a plateau becomes evident; indeed in almost all cases $m(T)$ is not useful for $T>2$. Hence we appeal to quenched simulations which indicate that for the "best" fuzzy wave functions even fits from $T=1$ to $T=2$ give reasonably accurate estimates for glueball masses and periodic flux loops [2,18]. In Figs. 3–5 we also show the fits obtained by using $m(2)$ in Eq. (4.1). As can be seen these mostly look reasonable bearing in mind that we know that the values of $C(T)$ at different T are strongly correlated and given our remarks about the likelihood of the errors at large T being underestimated. In some cases, e.g., Fig. 3(a), it is true that the apparent discrepancy between the fit and the data at larger T (between $T=2$ and 3 to be precise) is so large as to be worrying. As we shall see this is a good example of a situation where the $p\neq 0$ results will serve to reassure us.

As remarked above, we choose our "best" wave function by the standard variational criterion, i.e., the one that maximizes $C(1)/C(0)$ for a given state. We then take as our mass estimate the effective mass $m(2)$ extracted from the corresponding propagator. In practice, however, there are ambiguities with this simple procedure: different wave functions may possess values of $C(1)/C(0)$ that are equal within errors. Picking out one of these as better than the others is a procedure that is subjective and hence one which could introduce systematic biases. Accordingly we shall extract our mass estimates by doing simultaneous "correlated" fits between $T=1$ and 2 to all propagators whose values of $C(1)/C(0)$ are within one standard deviation of the maximum value found for this quantity.

In Table I we tabulate the values of $m(T)$ as obtained for the best zero-momentum 0^{++} operators on our various lattices. Table II does the same for the 2^{++} and Table III for the mass density of the periodic flux loop. This last quantity is, of course, just the string tension in lattice units (up to finite-volume corrections).

We can extract effective energies $E(T)$ from the $p\neq 0$ propagators in the same way as we extract $m(T)$ from the $p=0$ propagators. The values of these energies are tabulated in Tables IV–VI for the 0^{++}, 2^{++} glueballs and the flux loop, respectively.

To extract masses from the energies in Tables IV–VI we use the continuum dispersion relation

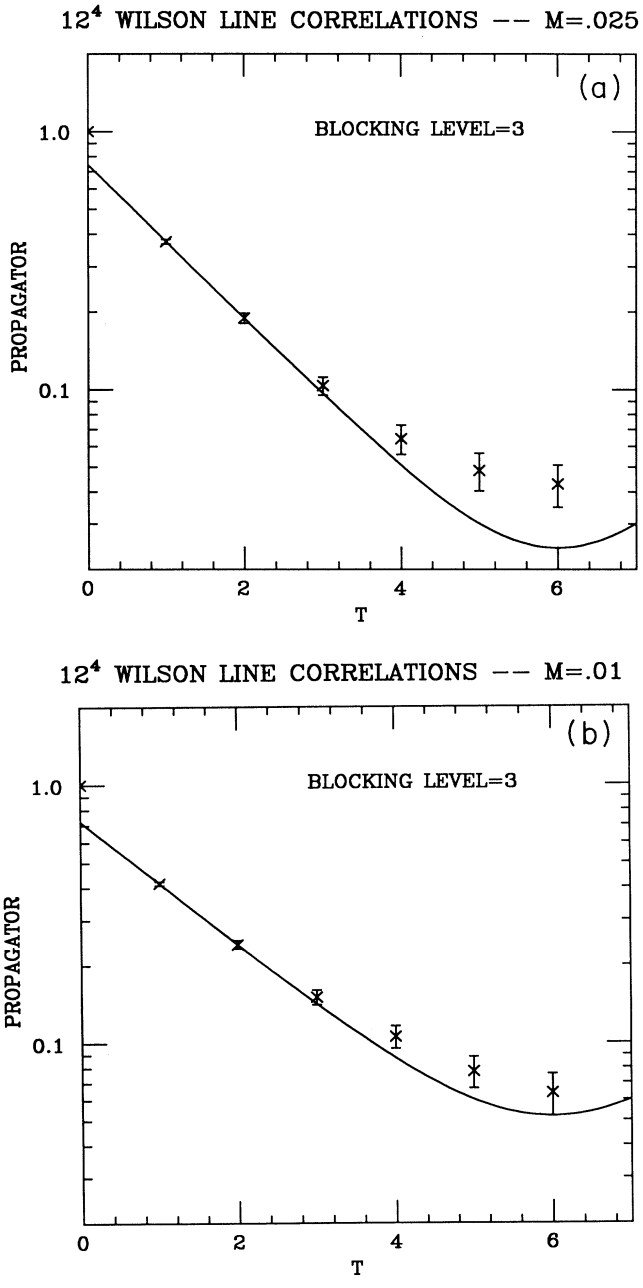

FIG. 5. The Wilson-Polyakov line correlation function on a 12^4 lattice: (a) $m_q=0.025$. Blocking level 3 on a logarithmic scale. The fit is to the form $0.7435\{\exp(-0.6863T)+\exp[-0.6863(12-T)]\}$ which fits the $T=1$ and $T=2$ data points. (b) $m_q=0.010$. Blocking level 3 on a logarithmic scale. The fit is to the form $0.7210\{\exp(-0.5536T)+\exp[-0.5536(12-T)]\}$ which fits the $T=1$ and $T=2$ data points.

TABLE I. The 0^{++} effective masses as a function of separation T. The states are as described in the text. The number in parenthesis after the state label indicates the blocking level. An asterisk indicates measurements from the "in-line code." Bold type indicates those states which obey the 1σ criterion.

			Effective masses			
m_q	Lattice	State	$T=0-1$	$T=1-2$	$T=2-3$	$T=3-4$
0.025	12^4	1×1 (2)	1.090 (25)	0.931(51)	0.652(89)	0.935(263)
		1×2 (2)	1.086(25)	0.861(61)	0.648(100)	0.914(263)
		8 link (2)	**1.025(25)**	**0.851(57)**	**0.612(81)**	**0.885(239)**
		1×1 (3)	1.087(31)	0.842(60)	0.566(71)	0.756(210)
0.010	12^4	1×1 (2)	1.058 (25)	0.939(66)	0.950(66)	1.208(795)
		1×2 (2)	1.054(30)	0.897(66)	0.864(159)	0.767(316)
		8 link (2)	**0.991(30)**	**0.851(60)**	**0.816(143)**	**0.770(276)**
		1×1 (3)	**0.995(34)**	**0.808(63)**	**0.825(151)**	**0.800(283)**
0.010	$12^3\times24$	1×1 (2)	1.074(64)	1.366(246)		
		1×2 (2)	1.078(63)	1.332(207)		
		8 link (2)	**1.036(56)**	**1.241(180)**		
		1×1 (3)	**0.983(60)**	**1.065(146)**		
0.010	16^4	1×1 (2)	1.064(41)	0.957(88)	0.881(252)	0.961(708)
		*1×1 (2)	1.090(30)	0.894(76)	0.977(228)	0.594(328)
		1×2 (2)	**1.039(38)**	**0.942(93)**	**0.856(221)**	**0.722(376)**
		8 link (2)	**1.005(35)**	**0.893(81)**	**0.854(187)**	**1.008(511)**
		1×1 (3)	1.063(33)	0.906(105)	0.878(188)	0.837(485)
		*1×1 (3)	1.087(31)	0.906(80)	0.875(211)	0.943(516)

TABLE II. The 2^{++} effective masses as a function of separation T. The states are described in the text. The number in parenthesis after the state label indicates the blocking level. An asterisk indicates measurements from the in-line code. Bold type indicates those states which obey the 1σ criterion.

			Effective masses		
m_q	Lattice	State	$T=0-1$	$T=1-2$	$T=2-3$
0.025	12^4	**1×1 (2)**	**1.738(33)**	**1.334(90)**	**0.971(296)**
		1×2*L* (2)	1.775(25)	1.470(107)	0.960(298)
		1×2*S* (2)	**1.730(32)**	**1.406(89)**	**0.875(245)**
		8 link (2)	**1.742(28)**	**1.279(89)**	**0.940(217)**
		1×1 (3)	1.790(35)	1.226(101)	1.029(206)
0.010	12^4	**1×1 (2)**	**1.717(29)**	**1.254(88)**	**1.473(444)**
		1×2*L* (2)	1.751(28)	1.271(72)	1.209(337)
		1×2*S* (2)	**1.733(29)**	**1.173(63)**	**1.704(431)**
		8 link (2)	1.767(36)	1.185(82)	1.713(476)
		1×1 (3)	**1.740(38)**	**1.130(92)**	**1.786(532)**
0.010	$12^3\times24$	**1×1 (2)**	**1.526(57)**	**0.816(168)**	**1.028(417)**
		1×2*L* (2)	**1.560(58)**	**0.712(148)**	**0.832(311)**
		1×2*S* (2)	**1.538(32)**	**0.765(156)**	**0.945(289)**
		8 link (2)	1.656(56)	1.062(220)	1.135(539)
		1×1 (3)	1.608(76)	0.732(144)	0.388(194)
0.010	16^4	**1×1 (2)**	**1.697(54)**	**1.439(190)**	**2.111(1397)**
		*1×1 (2)	1.747(37)	1.472(173)	1.502(686)
		1×2*L* (2)	**1.737(44)**	**1.518(172)**	**1.769(1059)**
		1×2*S* (2)	**1.705(45)**	**1.455(189)**	**1.452(814)**
		8 link (2)	1.772(45)	1.524(258)	0.858(441)
		1×1 (3)	1.867(57)	1.724(305)	0.493(516)
		*1×1 (3)	1.854(42)	1.389(164)	0.923(413)

TABLE III. The Wilson-Polyakov line effective masses per unit length, i.e., string tensions as a function of separation T. All measurements are at blocking level three. An asterisk indicates measurements from the in-line code.

		Effective masses per unit length					
m_q	Lattice	$T=0-1$	$T=1-2$	$T=2-3$	$T=3-4$	$T=4-5$	$T=5-6$
0.025	12^4	0.0818(18)	0.0572(23)	0.0518(34)	0.0455(42)	0.0393(53)	0.0415(128)
0.010	12^4	0.0731(15)	0.0461(18)	0.0418(24)	0.0370(33)	0.0416(42)	0.0534(83)
0.010	$12^3\times 24$	0.0640(21)	0.0402(28)	0.0305(34)	0.0294(51)	0.0197(60)	0.0227(67)
0.010	16^4	0.0932(15)	0.0612(40)	0.0520(64)	0.1056(458)		
	*	0.0945(16)	0.0665(30)	0.0625(109)	0.0505(215)	0.0759(862)	

$$E^2=m^2+p^2 \tag{4.3}$$

and this provides us with the effective masses tabulated in Tables VII–IX. Of course, even in the ideal case where Lorentz invariance has been effectively restored we should expect $O(a^2)$ lattice corrections to be present. Thus one might equally well have used in place of (4.3) the dispersion relation one obtains from the free field boson propagator; i.e.,

$$4\sinh^2(E/2)=4\sinh^2(m/2)+\sum_i 4\sin^2(p_i/2)\ . \tag{4.4}$$

On the 16^4 lattice the momenta are sufficiently small that using (4.4) would make little difference; even on the 12^4 lattice the (upward) shift in the masses is usually within the statistical errors. We have deliberately presented the raw energy values (in Tables IV–VI) so that the reader can use his own favorite variation on Eq. (4.3) in extracting the masses.

The utility of these $p\neq 0$ calculations is well illustrated by looking at the 0^{++} effective masses on the 12^4 lattice at $m_q=0.025$. As we previously saw in Fig. 3(a) and can now see in more detail in Table I, $m(T=3)$ appears to be considerably smaller than $m(T=2)$. However if we look in Table VII at the effective masses extracted from the lowest nonzero momentum, we see no such effect. This serves to reassure us that this apparent discrepancy is probably no more than a large statistical fluctuation.

There are several comments worth making again at this point. First, we recall the conclusions in the pure gauge case [18] that once the calculated statistical errors reach $\sim 15\%$ they become seriously unreliable. Second, we note that the errors along and between correlation functions are highly correlated: the correlation functions tend to fluctuate as a whole. Third, we remind the reader that because the distribution of $m(T)$ is not normal; a 2σ error (95%) is actually greater than twice the 1σ error (68%)—and very much greater once the error is large. This means that the effect of any underestimate of an already large error is usually greatly magnified.

In order to investigate whether all this is perhaps unduly alarmist, we have taken our longest runs, the 500 configurations on the 12^4 lattices at $m_q=0.01$ and 0.025, and have split them up into the first 240 and the last 260 configurations. In Figs. 6 and 7 we plot the effective 0^{++} and flux-loop masses obtained separately on these different subsets. We clearly see effects which confirm the necessity for caution.

Thus, given the nature of our statistical errors, we only feel confident in trusting our effective masses out to $m(2)$. Even here it is clear from Tables I–III that the low-statistics run on the $12^3\times 24$ lattice is behaving in a bizarre fashion. It is interesting to note that the masses extracted from the $p=2\pi/L$ propagators are in much better accord with what we see on the 12^4 and 16^4 lattices. Although the 16^4 lattice does not show any "anomalous" behavior it is clear that here too the statistics must be far from satisfactory. For example, when we examined separately the correlations of smeared Polyakov loops in the x, y, z directions and extracted string tensions from each we obtained the values $\kappa=0.0723(64)$, 0.0850(71), 0.0544(37), respectively; which shows that these correlation functions are sensitive to modes of the system whose relaxation times must be of the order of the

TABLE IV. 0^{++} effective energies.

			Energy (E)			
m_q	Lattice	State	$T=0-1$	$T=1-2$	$T=2-3$	$T=3-4$
			$p=(2\pi/L,0,0,E)$			
0.025	12^4	1×1 (2)	1.206(12)	1.047(30)	1.066(83)	0.923(204)
0.010	12^4	1×1 (2)	1.240(10)	1.037(25)	1.031(96)	0.691(123)
0.010	$12^3\times 24$	1×1 (2)	1.215(29)	0.953(75)	0.826(147)	0.753(316)
0.010	16^4	1×1 (2)	1.144(20)	0.905(40)	0.734(89)	0.683(147)
			$p=(2\pi/L,2\pi/L,0,E)$			
0.025	12^4	1×1 (2)	1.351(12)	1.163(43)	1.049(69)	1.029(233)
0.010	12^4	1×1 (2)	1.392(11)	1.213(42)	1.071(97)	1.334(404)
0.010	$12^3\times 24$	1×1 (2)	1.373(29)	1.180(98)	0.963(248)	0.416(331)
0.010	16^4	1×1 (2)	1.227(18)	1.001(43)	0.784(120)	0.783(236)

TABLE V. 2^{++} effective energies.

m_q	Lattice	State	Energy (E) $T=0-1$	$T=1-2$	$T=2-3$
			$p=(2\pi/L,0,0,E)$		
0.025	12^4	1×1 (2)	1.875(24)	1.466(74)	1.602(371)
0.010	12^4	1×1 (2)	1.825(17)	1.498(74)	1.105(233)
0.010	$12^3\times24$	1×1 (2)	1.859(60)	1.314(194)	0.996(573)
0.010	16^4	1×1 (2)	1.748(26)	1.356(99)	1.214(398)

total length of the run.

Although the tables give a good summary of our results it is useful to try to assign a single value to our 0^{++} and 2^{++} glueball masses for each lattice size and/or quark mass value. For this we shall combine the effective masses $m(2)$ from each wave function for which $m(1)$ is within one standard deviation of its minimum value. This is best done by simultaneously fitting one mass to each set of $T=1$ and $T=2$ data taking into account the fact that the propagators for these different wave functions are highly correlated. This gives

Lattice	m_q		From $p=0$	From $p=2\pi/L$
12^4	0.025	$M(0^{++})=$	0.85(6)	0.91(4)
		$M(2^{++})=$	1.34(8)	1.37(9)
		$\sqrt{\kappa(2)}=$	0.239(5)	0.256(4)
		$\sqrt{\kappa(3)}=$	0.228(7)	0.233(10)
12^4	0.010	$M(0^{++})=$	0.84(6)	0.89(3)
		$M(2^{++})=$	1.17(6)	1.41(8)
		$\sqrt{\kappa(2)}=$	0.215(4)	0.245(5)
		$\sqrt{\kappa(3)}=$	0.204(6)	0.225(10)
$12^3\times24$	0.010	$M(0^{++})=$	1.04(14)	0.79(10)
		$M(2^{++})=$	0.74(14)	1.20(22)
		$\sqrt{\kappa(2)}=$	0.200(7)	0.247(10)
		$\sqrt{\kappa(3)}=$	0.175(9)	0.239(25)
16^4	0.010	$M(0^{++})=$	0.86(8)	0.82(5)
		$M(2^{++})=$	1.50(16)	1.30(11)
		$\sqrt{\kappa(2)}=$	0.247(8)	0.253(8)
		$\sqrt{\kappa(3)}=$	0.228(14)	0.212(23)

(4.5)

where we also include values of the square root of the string tension, as extracted from both $T=2$ and $T=3$, in each case.

The most striking feature of all these numbers is their overall consistency. The only case that does not seem to fit is our low-statistics calculation on the $12^3\times24$ lattice. However, here we see a very large discrepancy between the masses extracted from $p=0$ and $p\neq0$, and indeed the $p\neq0$ masses do fit in with our other results. In view of this, we shall feel justified in disregarding the results from this lattice in our following discussions.

The consistency of these numbers suggest that the continuum hadron dispersion relations have apparently been restored, and that there is no strong dependence on either the quark mass or on the spatial volume. This last statement is also true of the more accurate effective masses extracted at $T=1$ (see Tables I–III).

As for glueballs other than the 0^{++} and the 2^{++}, their correlation functions fall rapidly into the noise indicating that either we have very poor wave functions or the states are heavy. There is some suggestion that several additional states, including the 0^{-+} might populate the region around twice the 0^{++} mass, or a little above, but higher statistics would be needed to resolve these.

Given that we have simultaneously calculated the ρ masses on all these lattices [11,12] it is tempting to use that information to give the glueball masses in GeV units. Since our glueball masses are not accurate enough to justify the sophistication of an extrapolation to the physical quark mass (presumably around $m_q=0.001$) we take ratios of our masses to the ρ mass and assume this ratio would not change if m_q was reduced. (Clearly such an assumption is poor, but even if we did have sufficient control over statistical and systematic errors to attempt such

TABLE VI. Periodic flux-loop effective energies.

m_q	Lattice	Blocking level	Energy (E) $T=0-1$	$T=1-2$	$T=2-3$	$T=3-4$	$T=4-5$
			$p=(2\pi/L,0,0,E)$				
0.025	12^4	2	1.378(12)	0.943(22)	0.835(44)	0.695(67)	0.558(99)
0.010	12^4	2	1.327(9)	0.889(24)	0.801(43)	0.807(111)	0.894(194)
0.010	$12^3\times24$	2	1.301(23)	0.899(51)	0.863(114)	1.365(343)	
0.010	16^4	3	1.647(25)	1.096(60)	0.819(131)	1.077(301)	
			$p=(2\pi/L,2\pi/L,0,E)$				
0.025	12^4	2	1.628(19)	1.173(43)	1.127(172)		
0.010	12^4	2	1.566(14)	1.103(32)	0.936(102)		
0.010	$12^3\times24$	2	1.620(56)	0.879(123)	1.102(181)		
0.010	16^4	2	1.917(43)	1.180(91)	0.787(222)		

TABLE VII. 0^{++} effective masses obtained from the effective energies of Table IV using the continuum dispersion relation.

m_q	Lattice	State	Eeffective mass $T=0-1$	$T=1-2$	$T=2-3$
			$p=(2\pi/L,0,0,E)$		
0.025	12^4	1×1 (2)	1.086(14)	0.907(34)	0.928(95)
0.010	12^4	1×1 (2)	1.124(11)	0.895(29)	0.888(111)
0.010	$12^3\times24$	1×1 (2)	1.096(32)	0.796(89)	0.639(190)
0.010	16^4	1×1 (2)	1.074(22)	0.815(45)	0.620(105)
			$p=(2\pi/L,2\pi/L,0,E)$		
0.025	12^4	1×1 (2)	1.130(15)	0.897(55)	0.742(97)
0.010	12^4	1×1 (2)	1.179(13)	0.961(53)	0.773(134)
0.010	$12^3\times24$	1×1 (2)	1.156(34)	0.918(126)	0.616(388)
0.010	16^4	1×1 (2)	1.094(20)	0.832(52)	0.553(170)

an extrapolation, it would be suspect. We say this, since simple extrapolations for the meson and nucleon masses using the data of Ref. [11] fail to produce a good N to ρ mass ratio. We invite the reader to use the data of this paper and Ref. [11] to perform his/her own extrapolations.) Setting the ρ to 770 MeV and using only our $m_q=0.01$ calculations we find

$$m(0^{++})=\begin{cases}1.2\pm0.1\pm0.2\ \text{GeV} & \text{for } L=12\ ,\\ 1.3\pm0.1\pm0.3\ \text{GeV} & \text{for } L=16\ ,\end{cases}$$

$$m(2^{++})=\begin{cases}1.7\pm0.1\pm0.3\ \text{GeV} & \text{for } L=12\ ,\\ 2.2\pm0.2\pm0.4\ \text{GeV} & \text{for } L=16\ ,\end{cases} \tag{4.6}$$

$$\sqrt{\kappa}=\begin{cases}300\pm10\pm60\ \text{MeV} & \text{for } L=12\ ,\\ 370\pm10\pm70\ \text{MeV} & \text{for } L=16\ ,\end{cases}$$

where the first error in each case is statistical and the second is our estimate of the systematic error from working at too large a quark mass. Since the error in m_N/m_ρ due to the large quark mass is approximately 20%, while that for the ρ mass (estimated from linear extrapolation) is about 10%, we estimate our systematic error from using this unphysical quark mass to be around 20%. The discrepancy between the $L=16$ and $L=12$ value of κ may be a finite volume effect, especially since we have seen evidence for finite-volume effects in the ρ to nucleon mass ratio in the $L=12$ case [11,12]. It is in the direction that one would expect [2] from the long-distance fluctuations of the confining string, i.e.,

$$\kappa(L)=\kappa(\infty)-\pi/(3L^2) \tag{4.7}$$

except that the effect is too large. The discrepancy between the values of κ derived from the $p=0$ and $p=\pi/6$ correlation functions lends further weight to this being a finite-size effect (the 12^4 value of $\sqrt{\kappa}$ from $p\neq0$ being ~350 MeV). In any case it is amusing to note that the string tension on the 16^4 lattice is close to the canonical value of around $(420\ \text{MeV})^2$, despite the fact that the phenomenological arguments for this value have never been very compelling. Finally, we note that for the 2^{++} glueball, the value of the mass we obtain from the $p\neq0$ correlations on the $L=12$ lattice is in fact consistent with the mass on the $L=16$ lattice. This suggests that the apparent discrepancies between the 2^{++} masses may also be due to finite-size effects.

Although we have been unable to resist the temptation of trying to translate the glueball masses into GeV units, we must emphasize that this procedure is fraught with systematic biases. For example, if we were to use the nucleon to set the scale, all our values in (4.6) would be reduced by almost 20% because our nucleon-to-ρ mass ratio is around 1.5 rather than the experimental value of about 1.22. This casts doubt on our cavalier assumption that the glueball-to-ρ mass ratio will remain approximately constant as the quark masses are decreased. Even if we had good reason to believe in the ρ rather than the nucleon, the substantial experimental width of the ρ must surely introduce an uncertainty of at least 10% in any mass scale we deduce from it. On the other hand the nucleon mass is harder to measure and appears [11,12] to exhibit significant finite-size effects.

TABLE VIII. 2^{++} effective masses obtained from the effective energies of Table V using the continuum dispersion relation.

m_q	Lattice	State	Effective mass $T=0-1$	$T=1-2$	$T=2-3$
			$p=(2\pi/L,0,0,E)$		
0.025	12^4	1×1 (2)	1.800(24)	1.369(79)	1.514(393)
0.010	12^4	1×1 (2)	1.748(18)	1.403(79)	0.973(265)
0.010	$12^3\times24$	1×1 (2)	1.784(62)	1.205(212)	0.847(674)
0.010	16^4	1×1 (2)	1.703(27)	1.298(103)	1.148(421)

TABLE IX. Effective string tensions obtained from the effective energies of Table VI using the continuum dispersion relation.

m_q	Lattice	Blocking level	Effective mass per unit length $T=0-1$	$T=1-2$	$T=2-3$	$T=3-4$
			$p=(2\pi/L,0,0,E)$			
0.025	12^4	2	0.1063(11)	0.0653(23)	0.0542(47)	0.0383(83)
0.010	12^4	2	0.1016(9)	0.0598(25)	0.0505(46)	0.0512(122)
0.010	$12^3\times 24$	2	0.0993(21)	0.0610(50)	0.0571(120)	0.1051(310)
0.010	16^4	3	0.1000(16)	0.0639(40)	0.0449(94)	0.0627(202)
			$p=(2\pi/L,2\pi/L,0,E)$			
0.025	12^4	2	0.1208(18)	0.0758(46)	0.0708(190)	
0.010	12^4	2	0.1150(14)	0.0681(36)	0.0478(139)	
0.010	$12^3\times 24$	2	0.1200(55)	0.0395(189)	0.0680(203)	
0.010	16^4	2	0.1147(28)	0.0650(63)	0.0348(196)	

V. TOPOLOGICAL CHARGE

For each gauge field configuration of the four sets of configurations mentioned above we have calculated the topological charge by the cooling method. As discussed in Sec. III this consists of locally smoothing each lattice gauge field configuration by locally minimizing its plaquette action. This is achieved by updating the configuration using a Cabibbo-Marinari heat bath with $\beta=\infty$.

How many cooling sweeps should one choose to perform? If the lattice spacing were very small, then this choice would not involve any ambiguity. Most of the lattice artifacts would be erased in the first few cooling sweeps and those that were not would, at this point, have linear extent $\rho\sim O(1)$ in lattice units. Thus they would be readily distinguishable, by direct inspection of the topological charge distribution on the cooled lattice, from the physical topological fluctuations with $\rho\sim O(\xi)$, where ξ is a typical dynamical length scale, e.g., the ρ Compton wavelength (hence $\xi\gg 1$). Since the (plaquette) action of such a narrow "instanton" is reduced when it shrinks, after at most a few further cooling sweeps we would expect all such artifacts to have shrunk out of the lattice. If we keep cooling beyond this point we would expect isolated topological fluctuations to begin to shrink very slowly since the instanton action is reduced by lattice spacing corrections that are of order $(1/\rho)^2$. Q itself should remain unchanged for the very large number of cooling sweeps required to shrink $\rho\sim O(\xi)$ to $\rho\sim O(1)$; at which point further cooling would expel from the lattice, one by one, what were originally the very broad topological charges. Eventually the configuration will be driven to the trivial field when the action is zero everywhere.

Of course, our calculations are nowhere near this ideal limit. The separation between physical and ultraviolet length scales is significant but is certainly not total. Hence, the best we can do is to choose some reasonable number of cooling sweeps that is neither too large nor too small, and check that the value of Q is insensitive to the precise number of cooling sweeps employed. Any ambiguities that are still left at this stage are hopefully small. In any case, whether small or not, they are "real" in the sense that they arise from the overlap between physical and ultraviolet length scales rather than being merely artifacts of the particular method.

Following previous quenched calculations [14] we have therefore calculated the topological charge after 5, 10, and 25 cooling sweeps. In Table X we show the corresponding values of $\langle Q^2\rangle$. These show, as hoped for, very little dependence on the number of cooling sweeps. This reflects the fact that for individual configurations Q rarely changes as we increase the number of cooling sweeps from 5 to 10 to 25. For example, on our 12^4 lattice at $m=0.01$ we find the following normalized correlation between the topological charge after 25 cools, $Q(25)$, and after j cools, $Q(j)$, where $j=5$ or 10:

$$\frac{\langle Q(25)Q(j)\rangle}{\langle Q(25)^2+Q(j)^2\rangle/2}=\begin{cases}0.92(2)\ , & j=5\ ,\\ 0.97(1)\ , & j=10\ .\end{cases} \tag{5.1}$$

In practice we shall choose the value of Q obtained after 25 cooling sweeps as an estimate of the topological charge of the original rough lattice gauge field.

As a further check, we take the configuration after 25 cooling sweeps and remove by hand any "instanton" whose core size is below some suitably chosen critical size. (We employ the same size criterion as in [14].) This gives us an estimate of the "large-scale" topological charge which we therefore label Q_{broad}. The difference between Q and Q_{broad} is some measure of the ambiguities remaining due to the lack of, as yet, a complete separation between physical and ultraviolet length scales.

An ambiguity of a much more trivial character arises from the fact that, due to well-understood order $(1/\rho)^2$ lattice corrections, the lattice topological charge is not exactly an integer. For a broad instanton it may be a few percent below $Q=1$ but for a very narrow charge the discrepancy may be much greater. Of course, such very narrow charges are rare in our calculations (as established by our above checks and comparisons) and can in any case be easily identified in the cooled configuration. Since there is no reason to believe that the deviation from integer values on the cooled lattices is any measure at all of lattice artifact contributions in the original "hot" lattices we round the value of Q to the appropriate integer.

That this procedure is unambiguous in our case is illustrated in Fig. 8 where we plot the histograms of the measured charges, before rounding, and observe that they do indeed cluster near integer values. For the rare cases that lie between the peaks, looking directly at the topological charge density distribution on the cooled lattice almost always resolves the apparent ambiguity.

Plotting the time evolution of the topological charge, in Fig. 9, we notice that there are obvious fluctuations with a long relaxation time, especially in the data for $m_q=0.010$ on a 12^4 lattice. Indeed, we see in the severe skewing of the distribution of Q values in Fig. 8(a) more

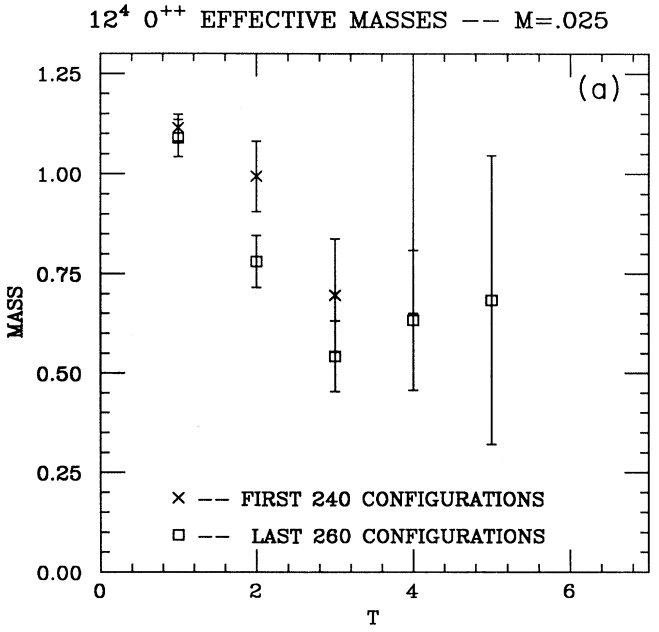

FIG. 6. (a) A comparison between the 0^{++} effective masses measured from the first 240 and last 260 configurations on a 12^4 latice with $m_q=0.025$. (b) A comparison between the effective string tensions measured from the first 240 and last 260 configurations on a 12^4 lattice with $m_q=0.025$.

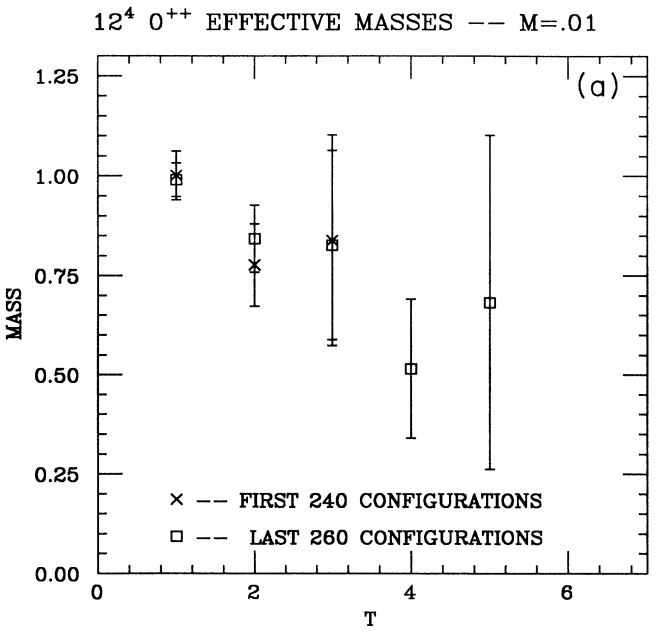

FIG. 7. (a) A comparison between 0^{++} effective masses measured from the first 240 and last 260 configurations on a 12^4 lattice with $m_q=0.010$. (b) A comparison between the effective string tensions measured from the first 240 and last 260 configurations on a 12^4 lattice with $m_q=0.010$.

evidence for such an effect. Thus in order to calculate errors in $\langle Q^2 \rangle$ we bin the data into bins that are as large as possible while still maintaining a reasonably large number of bins, i.e., into bins of 20 configurations for the two 12^4 runs, and into bins of 5 configurations for the $12^3 \times 24$ and the 16^4 runs. To further investigate the possible long-time fluctuations in this quantity we divide each of the sets of 25 bins of our data into the first 12 bins and the last 13 bins. We find the pattern

Lattice	m_q	$\langle Q^2 \rangle$ First half data	$\langle Q^2 \rangle$ Second half data
12^4	0.025	2.17(31)	1.74(28)
12^4	0.010	1.93(43)	0.79(16)
16^4	0.010	5.48(109)	3.40(82)

(5.2)

In every case there is a reduction in the latter half of the

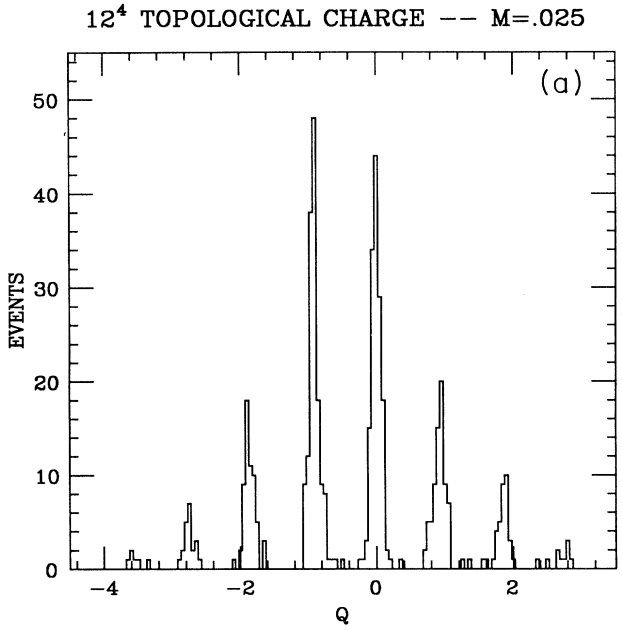

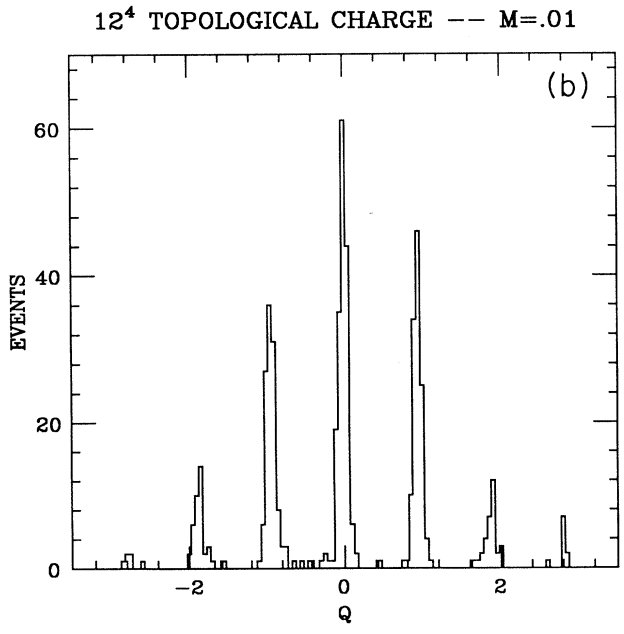

FIG. 8. Histograms of the distribution of topological charge Q measured on a 12^4 lattice (a) for the 500 configurations with $m_q = 0.025$; (b) for the 500 configurations with $m_q = 0.010$.

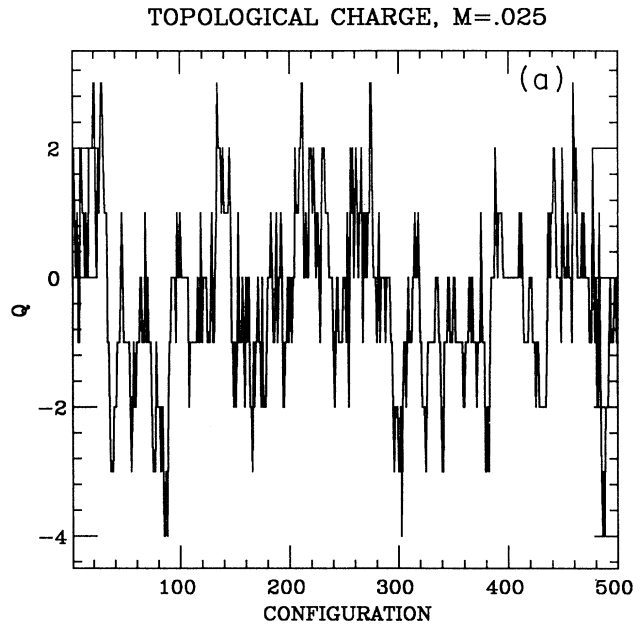

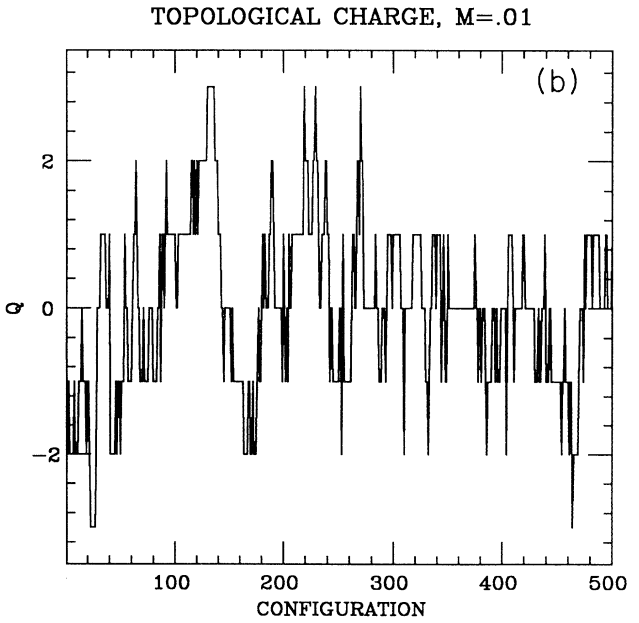

FIG. 9. Time evolution of topological charge on a 12^4 lattice (a) for $m_q = 0.025$; (b) for $m_q = 0.010$.

run. The effect is only at the level of 1, 2.5, and 1.5σ, respectively, in the three cases, so while it does suggest that the topological charge is sensitive to very long-range correlations in the system (and hence that our errors may well be underestimated) it would be useful to have some measure of topological fluctuations that is less noisy than Q^2.

To construct such a measure we follow [19] and define the quantity

$$\tilde{Q}=\sum_n |Q(n)| \ , \tag{5.3}$$

where $Q(n)$ is the topological charge density on site n. On cooled lattices this is clearly a measure of the (long distance) topological activity of the vacuum. Indeed, if we assume the strict dilute-gas approximation and if we also assume that the lattice spacing is small enough for the cooling not to have caused any significant annihilation amongst neighboring instantons and anti-instantons, then we can easily show that

$$\langle \tilde{Q} \rangle = \langle Q^2 \rangle \ . \tag{5.4}$$

Of course, because of the presence of partially annihilated instanton anti-instanton pairs, $\tilde{Q}$ will, unlike Q, have no reason to take values close to integers. So, if after 25 cooling sweeps we calculate $\tilde{Q}$ we find the pattern

		$\langle \tilde{Q} \rangle$	
Lattice	m_q	First half data	Second half data
12^4	0.025	2.61(9)	2.23(12)
12^4	0.010	1.96(6)	1.71(9)
16^4	0.010	6.86(23)	6.08(22)

(5.5)

We see that, once again, we have in every case a reduction in the latter half of the run: moreover, it is now at the 2.5σ level in each case. This provides stronger evidence that the modes of the system with large spatial extent which are probed by measurements of global topology, have relaxation times of the order of the total length of our runs (if not longer), and thus, cannot be considered to have equilibrated. While this is not good news, we can be somewhat reassured by the fact that although this effect is visible, the variation we observed in (5.5) is quite small in absolute terms.

In Ref. [19] the quantity $\tilde{Q}$ was, in fact, used as a sensitive probe of finite-size effects. It is interesting to repeat this analysis on our calculations. One defines a "pseudosusceptibility" $\tilde{\chi}$ as

$$\tilde{\chi}=\langle \tilde{Q} \rangle / V \tag{5.6}$$

and compares the values on lattices of different sizes but with the same values of the couplings. As argued in Ref. [19], $\tilde{\chi}$ should be the same on such lattices insofar as finite-volume effects are negligible. If we calculate this quantity on our 12^4 and 16^4 lattices with $m_q=0.010$ and compare with the quenched ($m_q=\infty$) value at $\beta=5.9$ [19] (the quenched value of β at which the hadron spectrum most closely reproduces the spectrum on our lattices) we find

	$\tilde{\chi}\times 10^4$	
Lattice	$\beta=5.9; m_q=\infty$	$\beta=5.6; m_q=0.010$
8^4	0.93(11)	
10^4	1.46(8)	
12^4	1.498(22)	0.884(29)
16^4	1.498(22)	0.984(27)

(5.7)

In contrast with the pure gauge case there is a significant change in $\tilde{\chi}$ as we go from the 12^4 to the 16^4 lattice. This confirms the hints of finite-volume effects that we had earlier, from the values of the string tension on these lattices. Indeed, the above comparison suggests that in QCD with two light quarks finite-volume effects begin to become important on volumes that are about 1.3–1.5 the size on which equivalent effects set in, in the pure gauge theory. Note that this is certainly consistent with what we know about the scales of the deconfining phase transition in the two theories.

From the value given in Table X, our topological susceptibility

$$\chi=\langle Q^2 \rangle / V \tag{5.8}$$

takes the following values in lattice units:

Lattice	m_q	χ
12^4	0.025	$9.4(10)\times 10^{-5}$
12^4	0.010	$6.5(11)\times 10^{-5}$
$12^3\times 24$	0.010	$7.7(14)\times 10^{-5}$
16^4	0.010	$6.7(10)\times 10^{-5}$

(5.9)

Note the agreement between the three different lattice sizes at $m_q=0.010$, albeit within the substantial errors.

Let us now consider whether these values are con-

TABLE X. Topological susceptibility as a function of the number of cooling sweeps. The last column is the result of removing by hand narrow instantons, as in [14,18], after 25 cooling sweeps.

m_q	Lattice	5 cools	10 cools	25 cools	Broad
0.025	12^4	1.94(21)	1.93(21)	1.95(21)	1.56(19)
0.010	12^4	1.40(25)	1.33(24)	1.34(24)	1.21(23)
0.010	$12^3\times 24$	3.29(59)	3.34(57)	3.21(58)	2.97(58)
0.010	16^4	4.39(78)	4.54(78)	4.40(68)	3.14(53)

sistent with the theoretical predictions of Eq. (3.5). First let us argue that we are in the large-volume region. We suspect that this is so, since even for our smallest lattice (12^4) and smallest quark mass ($m_q=0.01$), $m_\pi L \approx 3.2 \gg 1$. To make this more precise we need to argue that $f_\pi^2 m_\pi^2 V \gg 1$. We calculate f_π from

$$f_\pi^2 m_\pi^2 = m_q \langle \bar{\psi}\psi \rangle \tag{5.10}$$

where in this and subsequent equations we have used $n_f=2$ and $\langle \bar{\psi}\psi \rangle$ has been extrapolated linearly to $m_q=0$. This yields $f_\pi=0.0535(13)$ from the 12^4 lattice. Note that if we were to use the ρ mass also extrapolated to $m_q=0$ as our scale, we would obtain $f_\pi=85(3)$ MeV which as expected lies slightly below the true value $f_\pi=93$ MeV, but close enough to give us some faith in our estimates. For the worst case ($m_q=0.01$ on a 12^4 lattice) we find $f_\pi^2 m_\pi^2 V \approx 4.2 \gg 1$ so that we are indeed in the large-volume regime.

Following Ref. [17] we can estimate the finite-volume corrections to $\langle \bar{\psi}\psi \rangle$. This predicts a 13% decrease at $m_q=0.01$ on a 12^4 lattice, a 2% decrease at $m_q=0.01$ on a 16^4 lattice and a 2% decrease on a 12^4 lattice at $m_q=0.025$. At $m_q=0.01$ we have a more direct measure of these finite-volume effects, the measured values of $\langle \bar{\psi}\psi \rangle$ which are 0.0549(6) for the 12^4 lattice and 0.0569(5) for the 16^4 lattice. Although the difference is in the right direction, the actual magnitude is much less than the above estimates. One of the reasons for this is that the Hansen-Leutwyler formulas assume flavor symmetry, in the form of degenerate pions. At $\beta=5.6$, this is not yet achieved. For our calculations we used the mass of the lightest (Goldstone) pion. On the 12^4 lattice at $m_q=0.01$ this is $m_\pi=0.2663(30)$. However, we have also calculated a second pion mass on this lattice with $m_\pi=0.349(12)$. Had we use this mass instead, the predicted 13% would decrease to 4%. Whatever the reason, the finite-volume effects are small enough that it is safe to extrapolate $\langle \bar{\psi}\psi \rangle$ to $m_q=0$, and use the small m_q prediction

$$\chi = \frac{m_q}{4} \langle \bar{\psi}\psi \rangle \tag{5.11}$$

which gives

$$\begin{aligned} &m_q=0.025\ , \quad \chi=12.7(6)(3)\times 10^{-5}\ , \\ &m_q=0.010\ , \quad \chi=5.1(3)(1)\times 10^{-5}\ , \end{aligned} \tag{5.12}$$

where the first error is statistical, the second our estimate of the finite-volume effects we have neglected.

If we compare the theoretical predictions in Eq. (5.12) with our calculated values in Eq. (5.9) there are two features that stand out. The first is the remarkable agreement at the smaller quark mass. The second is that the calculated quantities appear to possess a much weaker mass dependence than the linear one that we expect to find at sufficiently small m_q. Indeed the ratio of the susceptibilities calculated at $m_q=0.025$ and $m_q=0.010$ is 1.46(30) rather than the 2.5 that a linear dependence would give us. Of course, considering the fact that we have presented evidence that there are such long-time correlations in our measurements of Q, that the statistical errors quoted in Eq. (5.9) are almost certainly underestimates, the agreement between the measured values χ given in Eq. (5.9) and the predicted values of Eq. (5.12) is remarkably good. If the apparent discrepancies between (5.9) and (5.12) are real, they could well be due to finite lattice size and/or spacing effects, or the terms quadratic in m_q. Included in these terms of higher order in m_q are those involved in extrapolating $\langle \bar{\psi}\psi \rangle$ to zero mass, which are also those terms involved in defining a renormalization scheme for Eq. (3.5). Nonetheless if we had seen a linear m_q dependence this would have served to reassure us that the agreement at the lowest mass, $m_q=0.010$, was no accident. Without such reassurance we must remain cautious.

VI. MIXING

Since the vacuum has light-quark loops, the confining string will break once it is long enough, and it is not clear that there will be any flux loop from which to extract the string tension. Similarly, glueballs will mix with $q\bar{q}$ mesons. Our calculations, on the other hand, have used purely gluonic wave functions and have extracted masses from the small-distance correlations of the best such operators. It is therefore clear that these "masses" can only be what they purport to be if the states are indeed largely gluonic and the mixing is weak. What is our evidence for this?

To probe this question directly we would need to have calculated the overlaps between the "best" glueball and mesonic wave functions and also between our flux loop operators and appropriate glueball, mesonic, and vacuum states. Unfortunately, while we hope to carry out such calculations in the future, in the present calculations we have only obtained the overlaps onto the vacuum state. To extract the most from this limited information we shall have to supplement what we know with what we suppose. The upshot of this exercise will be that mixing is not important. However, it must be emphasized that all this leaves plenty of scope for surprises. We begin with the flux loops and the string tension.

Our smeared Polyakov loop operators are designed to create excitations that are similar to the lowest-mass periodic flux loop in the pure gauge theory. As such an excitation propagates from one operator of the correlation function to the other, it may be broken by the excitation of a $q\bar{q}$ pair somewhere along its length. If this $q\bar{q}$ pair immediately reannihilates then all this will do is to modify the value of the string tension and perhaps the shape of the wave function. To make a qualitative difference the $q\bar{q}$ pair has to separate by a distance that is comparable to the length of the flux loop so as to turn the periodic flux loop into a local state. If the $q\bar{q}$ pair annihilates at this point then the flux loop will mix with the vacuum or with glueball states. If not, it will mix with meson states. (One can straightforwardly generalize this discussion to the case where several $q\bar{q}$ pairs may be formed, which would be appropriate for a very long flux loop on a very large lattice.) In all these cases, the $q\bar{q}$ pair

has to separate over distances $>O(1\text{ fm})$ and so it is the "constituent" quark mass that is appropriate. Phenomenologically, processes involving the production and annihilation of long-distance $q\bar{q}$ pairs seem relatively small. Hence the common assumption is that mixing between gluonic and mesonic states should be weak. It is worth adding, however, that if the dynamics does not suppress mixing then we should certainly not expect to receive any help from the kinematics: the apparent flux-loop mass falls in the range 0.55 (on 12^4 at $m_q=0.010$) to 1.07 (on 16^4 at $m_q=0.010$) which means there are plenty of nearby states with which to mix.

So much for the background; what do our calculations indicate? As stated above, we have only calculated explicitly the overlap between the flux loop wave functions and the vacuum. To present the results in a physically meaningful form we calculate the normalized overlap

$$A=\frac{|\langle \text{vac}|P|\text{vac}\rangle|^2}{\sum_n[|\langle \text{vac}|P|n\rangle|^2]}\ , \tag{6.1}$$

where P is our best smeared zero-momentum Polyakov loop wave function. Our results are

Lattice	m_q	A
12^4	0.025	<0.0015
12^4	0.010	<0.0075
$12^3\times 24$	0.010	<0.0082
16^4	0.010	<0.0006

(6.2)

These overlaps are quite remarkably small; we recall that the overlaps of this operator on to the lightest loop states are typically of the order 0.7–0.9. This is in complete contrast to the case of glueballs where the quantity A for the best (vacuum unsubtracted) 0^{++} glueball operator is close to 1. So the suppression we are observing here must be due to a corresponding suppression of the $q\bar{q}$ creation and annihilation since this is involved in the vacuum overlap of the flux loop but not in that of the glueball. (Remember that in the confined phase of the quenched theory, global Z_3 symmetry prevents the flux loop from having any vacuum overlap.) This is not only providing us interesting corroboration of the phenomenological observation that long-distance $q\bar{q}$ vacuum fluctuations are unimportant, but is simultaneously telling us that the mixing of flux loops with the vacuum and glueball states is negligible.

If $q\bar{q}$ fluctuations are small then we would expect overlaps between the flux loops and meson states to be on the order of the square root of their overlaps onto the vacuum. So we expect

$$\text{flux-loop–meson overlap } <10\%\ . \tag{6.3}$$

It is interesting to note that the apparent overlap of our best operator onto the lightest flux loop state is about 5–10% less on our 12^4 QCD lattice than it was in the pure gauge case on the same lattice.

While the above estimates are far from watertight they do lead us to believe that the flux loops are not severely perturbed by the presence of light vacuum quarks and that what we have extracted in indeed the quantity that corresponds, phenomenologically, to the string tension.

As far as the glueballs are concerned, we have no information on the mixing with mesons except for the observation that the overlap of the best glueball wave functions onto the (apparently) lightest glueball states are very similar to the 0.8–0.9 values obtained in the pure gauge theory at comparable values of the lattice spacing and that they display no obvious dependence on the quark mass. This would be consistent with a mixing estimate similar to that in (6.3),

$$\text{glueball-meson overlap } <10\%\ , \tag{6.4}$$

in which case our glueball mass estimates should also be quite reliable.

VII. CONCLUSIONS

Perhaps the most informative way to summarized our results is to compare our calculated masses with the meson and baryon masses that we have reported elsewhere [11,12] (see Fig. 10). It is also interesting to compare these results with a comparable plot obtained on a 12^4 lattice at $\beta=5.9$ in the pure gauge theory (which happens to possess a lattice spacing that is comparable to the one in our QCD calculations).

We only show the 0^{++} and 2^{++} glueball masses. The masses of states with other J^{PC} assignments appear to be considerably larger (or, as is the case with the 0^{-+}, too noisy for us to make an estimate). Unfortunately glueballs with "oddball" quantum numbers appear so heavy as to be of little experimental interest. It has to be emphasized, however, that states which appear heavy are particularly susceptible to lattice-spacing corrections and all these conclusions need corroboration on lattices with much smaller lattice spacings (which is not going to happen soon).

If we use the ρ to set the scale in laboratory units we obtain

$$\begin{aligned} &m(0^{++})=1.2-1.3\pm0.1\pm0.3\text{ GeV}\ ,\\ &m(2^{++})\sim 1.5m(0^{++})=1.7-2.2\pm0.2\pm0.4\text{ GeV}\ ,\\ &\sqrt{\kappa}=0.30-0.37\pm0.01\pm0.07\text{ GeV}\ , \end{aligned} \tag{7.1}$$

where, as in (4.7), the first error is statistical, the second systematic. If we were to use the nucleon, then these numbers would drop by about 20%. (Here we note that we have provided plenty of evidence that these statistical errors are probably underestimated.)

Given the theoretical uncertainties in the customary phenomenological extraction of a value for the string tension, it is actually quite interesting that our value is not at all far from the "canonical" $(420\text{ MeV})^2$.

The lightest glueball masses occupy what is phenomenologically an interesting mass range. Of course, all our masses have been calculated under the assumption that mixing is suppressed and our direct evidence for this, in the form of (a) the remarkably strong suppression of the

overlap between periodic flux loops and the vacuum, and (b) the fact that the overlaps onto the (apparently) lightest states are large and comparable to the pure gauge case, clearly needs improving upon in subsequent calculations. Higher statistics enabling us to observe if we have a plateau in the effective mass would help. Nonetheless, point (a) provides nice direct evidence for the suppression of quark loop effects on physical length scales.

If we accept our limited evidence that $q\bar{q}$ mixing has little effect on glueballs and the confining string, it is tempting to question whether reducing the value of the quark mass from our value of $m_q=0.01$ to the physical value of about $m_q=0.001$, can possibly alter the qualitative features of the picture we have obtained. The reason is that, as we see in Fig. 10, the glueball states are already more massive than some mesonic states with the same quantum numbers and, moreover, the "constituent" quark mass is not expected to alter greatly when we

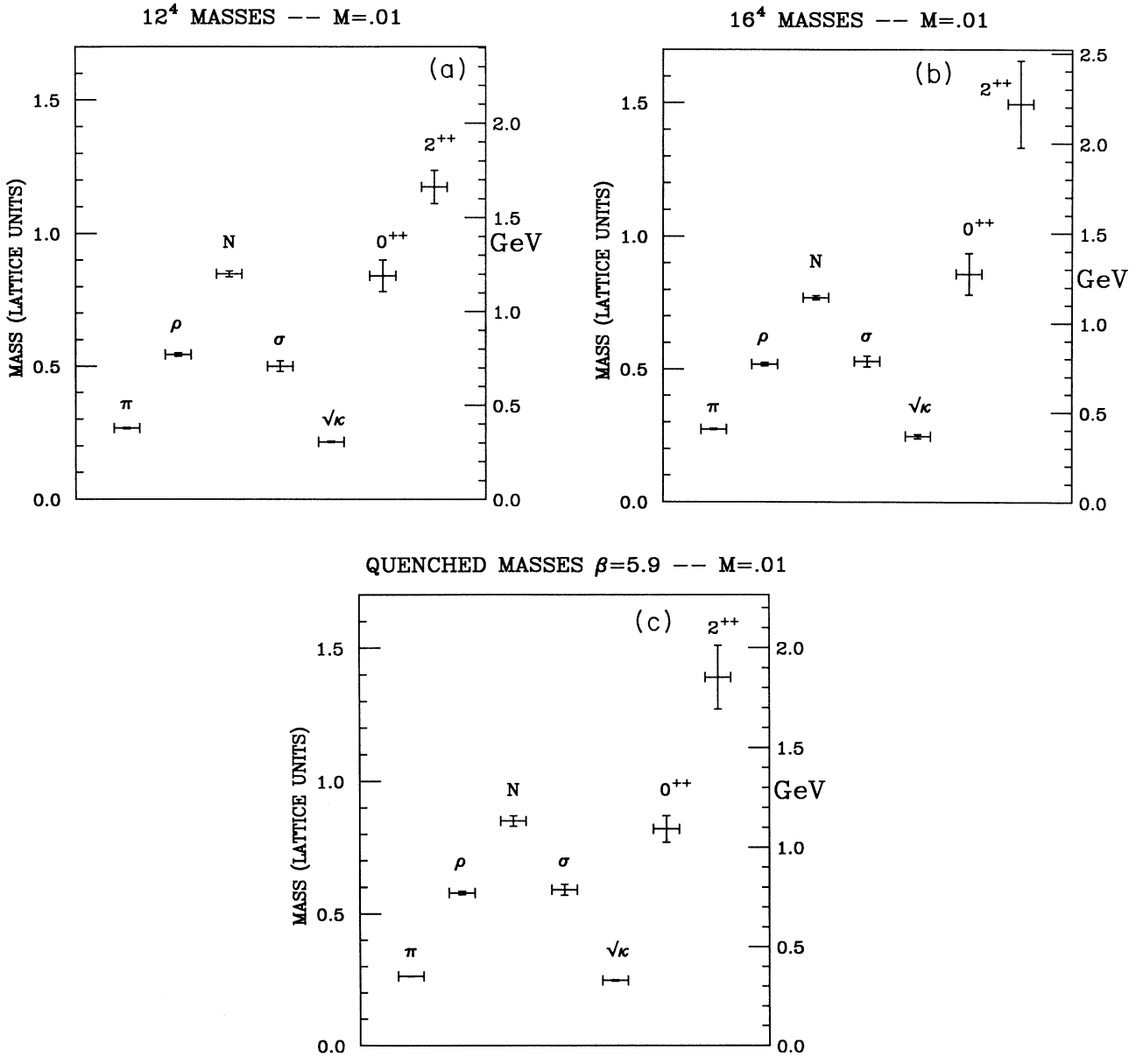

FIG. 10. (a) The $12^4 m_q=0.010$ 0^{++} and 2^{++} glueball masses and the square root of the string tension compared with meson and baryon masses measured on the same configurations. (b) The $16^4 m_q=0.010$ 0^{++} and 2^{++} glueball masses and the square root of the string tension compared with meson and baryon masses measured on the same configurations. (b) 0^{++} and 2^{++} glueball masses and the square root of the strong tension compared with meson and baryon masses (for valence quark mass $m_q=0.010$) measured on quenched 12^4, respectively, $16^3\times 32$ lattices at $\beta=5.9$.

reduce the bare mass m_q any further. Of course, lowering m_q will make the pions much lighter and thus enhance the "decay" of our glueballs into multipion states. However, even at the present pion mass, "decays" into few pion states are already kinematically allowed.

It is clear that, as far as the gluonic sector of the theory is concerned, what we really need is much higher statistics. We also need the direct calculations of glueball-$q\bar{q}$ mixings that would become possible in such calculations. We might then be able to see variations of the spectrum with m_q which are simply not visible with our very crude data. It would also be useful to get away from the uncertainties adhering to our statistical errors and possible lack of equilibration.

Unfortunately, what we appear to need most for the gluonic sector clashes with what we appear to need most in the hadronic sector, i.e., smaller m_q, smaller lattice spacings and larger lattices. This is because one finds, as usual in these calculations, that the determination of hadron propagators is remarkably accurate when compared to that of the gluonic states. It is presumably the case that if we were calculating hadrons in the same way as we calculate glueballs, i.e., generating directly the pseudo-Grassman fields and calculating directly the correlations of appropriate color-singlet products of these field variables, we would obtain similarly noisy correlators. Calculating quark propagators in a background gauge field yields the effect of integrating out all these fermion fields, i.e., of doing a complete fermion simulation in a fixed gluonic background. This produces the exponential behavior of hadronic propagators from a single configuration thus greatly reducing the number of configurations needed for accurate measurements. What we really need is a glueball method that more closely resembles that for hadrons.

Better statistics from longer runs are also needed to measure the mass dependence of the topological susceptibility to compare with theory, in both the chirally broken and chirally symmetric phases. The weaker than expected mass dependence from the present calculations is inconclusive. Some evidence of the correctness of the predicted mass dependence has been obtained in simulations of the SU(2)-four-flavor theory. In this SU(3)-two-flavor theory, such a measurement is more important, since observing the predicted mass dependence in both phases would give evidence that the flavor tuning required to give two flavors has indeed produced two flavors with the correct anomaly structure. That the latter is indeed the case receives some support from the fact that the magnitude of our susceptibility at the smallest quark mass is in good agreement with the predictions of the $n_f=2$ anomalous Ward identity.

Finally, we remark that, as in all lattice QCD calculations to date, the quark masses are too large, the lattice sizes too small, and the coupling too large to access the entire physical continuum limit. However, if quenched simulations are taken as a guide, which might be a reasonable thing to do if the mixing between the lightest glueballs and mesons is relatively small and these glueballs exist as narrow states, then it is not impossible that the kind of exploratory calculation we have described in this paper should give a recognizable picture of the true level pattern.

ACKNOWLEDGMENTS

This work was supported under U.S. Department of Energy Contracts No. DE-FG02-85ER-40213, No. DE-AC02-86ER-40253, No. DE-AC02-84ER-40125, No. DE-AS03-81ER-40029, No. DE-FC05-85ER250000, and No. W-31-109-ENG-38 and by National Science Foundation Grants No. NSF-PHY87-01775, No. NSF-PHY89-04035, and No. NSF-PHY86-14185. The computations were supported under a Department of Energy Grand-Challenge Grant at the Florida State University Supercomputer Research Institute which is partially funded by the U.S. Department of Energy through Contract No. DE-FC05-85ER250000.

[1] Particle Data Group, J. J. Hernández *et al.*, Phys. Lett. B **239**, 1 (1990).
[2] C. Michael and M. Teper, Nucl. Phys. **B314**, 347 (1989).
[3] The APE Collaboration, M. Albanese *et al.*, Phys. Lett. B **197**, 400 (1987).
[4] T. A. DeGrand, Phys. Rev. D **36**, 176 (1987); **36**, 3522 (1987).
[5] A. A. Belavin, A. M. Polyakov, A. S. Schwartz, and Yu. S. Tyupkin, Phys. Lett. **59B**, 85 (1975).
[6] S. Coleman, in *The Whys of Subnuclear Physics,* Proceedings of the International School, Erice, Italy, 1977, edited by A. Zichichi, Subnuclear Series Vol. 15 (Plenum, New York, 1979).
[7] G. 't Hooft, Phys. Rev. Lett. **37**, 8 (1976); Phys. Rev. D **14**, 3432 (1976).
[8] E. Witten, Nucl. Phys. **B156**, 269 (1979). G. Veneziano, *ibid.* **B159**, 213 (1979); Phys. Lett. **95B**, 90 (1980).
[9] C. Callan, R. Dashen, and D. Gross, Phys. Rev. D **17**, 2717 (1978); **19**, 1826 (1979). For a recent quenched investigation, see S. Hands and M. Teper, Nucl. Phys. **B347**, 819 (1990).
[10] J. B. Kogut, D. K. Sinclair, and M. Teper, Nucl. Phys. **B348**, 178 (1991).
[11] K. M. Bitar, T. A. DeGrand, R. Edwards, S. Gottlieb, U. M. Heller, A. D. Kennedy, J. B. Kogut, A. Krasnitz, W. Liu, M. C. Ogilvie, R. L. Renken, P. Rossi, D. K. Sinclair, R. L. Sugar, M. Teper, D. Toussaint, and K. C. Wang, Phys. Rev. D **42**, 3794 (1990).
[12] K. M. Bitar, T. A. DeGrand, R. Edwards, S. Gottlieb, U. M. Heller, A. D. Kennedy, J. B. Kogut, A. Krasnitz, W. Liu, M. C. Ogilvie, R. L. Renken, P. Rossi, D. K. Sinclair, R. L. Sugar, M. Teper, D. Toussaint, and K. C. Wang, Phys. Rev. Lett. **65**, 2106 (1990).
[13] M. Teper, Phys. Lett. B **183**, 345 (1987).
[14] M. Teper, Phys. Lett. **162B**, 357 (1985); J. Hoek, M. Teper, and J. Waterhouse, Nucl. Phys. **B288**, 589 (1987).
[15] The APE Collaboration, M. Albanese *et al.*, Phys. Lett. B **192**, 163 (1987).
[16] T. A. DeGrand and C. Peterson, Phys. Rev. D **34**, 3180 (1986).
[17] F. C. Hansen and H. Leutwyler, Nucl. Phys. **B350**, 201 (1991).
[18] C. Michael and M. Teper, Phys. Lett. B **206**, 299 (1988).
[19] M. Teper, Phys. Lett. B **202**, 553 (1988).